JOURNAL OF SPACECRAFT AND ROCKETS
Vol. 41, No. 4, July–August 2004

Dynamics of the Active Plasma Experiment North Star Artificial Plasma Jet

P. A. Delamere*
University of Colorado, Boulder, Colorado 80309-0391
H. C. Stenbaek-Nielsen†
University of Alaska Fairbanks, Fairbanks, Alaska 99775-7320
R. F. Pfaff‡
NASA Goddard Space Flight Center, Greenbelt, Maryland 20771
R. E. Erlandson§ and C. I. Meng¶
Johns Hopkins University, Applied Physics Laboratory, Laurel, Maryland 20723
and
J. I. Zetzer,** Y. Kiselev,†† and B. G. Gavrilov‡‡
Institute for Dynamics of Geospheres, 117979, Moscow, Russia

Active Plasma Experiment North Star was launched from Poker Flat Research Range, Alaska, on 22 January 1999 at 13:57:03 UT, with two explosive-type generators that produced an artificial aluminum plasma jet. The purpose of this experiment was to study the interaction of the artificial plasma jet with the ambient plasma. The first release occurred at 363 km, and a ∼90% reduction of the geomagnetic field was observed on three separate daughter payloads. The diamagnetic signatures suggest that the plasma cloud was highly localized (i.e., cloud dimensions ∼Al^+ gyroradius) traveling with a velocity of roughly 25 km/s perpendicular to the geomagnetic field. A hybrid code simulation provided an estimate of the plasma distribution and a qualitative description of the evolution of the plasma cloud. The simulation showed that the plasma cloud polarized and $\boldsymbol{E} \times \boldsymbol{B}$ drifted while transferring momentum to the ambient plasma via an Alfvénic disturbance. The model results are in good qualitative agreement with data from the plasma diagnostics payload.

Nomenclature

A = perpendicular cross section
$\boldsymbol{B}$ = magnetic field vector
$\boldsymbol{E}$ = electric field vector
L = field-aligned length scale
m = mass
N = number of particles
n = density
p = momentum
t = time
$\boldsymbol{u}$ = fluid bulk flow velocity vector
V = volume
v = velocity
τ = momentum transfer time scale

Subscripts

A = Alfvén
c = cloud
e = electrons
f = fluid
i = ions
p = particle
r = radial
T = transferred momentum/properties of the ambient medium
th = thermal velocity
0 = initial value

Introduction

PLASMA injection experiments have been employed to study a variety of plasma phenomena in the Earth's ionosphere and magnetosphere. An intriguing application for active experiments is the long-standing and complex problem of momentum coupling between a partially ionized gas moving relative to an ambient magnetized plasma.[1] An obvious example of such a system is the neutral atmosphere and gas clouds of Jupiter's moon, Io, interacting with the corotating Io plasma torus. Other examples include cometary gas clouds interacting with the solar wind and coronal mass ejections. Moreover, auroral emissions at the base of Io's flux tube suggest that electron acceleration might be a consequence of an Alfvénic interaction.[2–4] Hence, a detailed understanding of active plasma experiments can have general application to electron acceleration processes. The Active Plasma Experiment (APEX) North Star provided a unique opportunity to investigate the interaction between an ionized aluminum jet and the Earth's ionospheric plasma environment.

Previous experiments include a series of barium releases, which were conducted at a variety of altitudes in the Earth's ionosphere and magnetosphere as a part of the Combined Release and Radiation Effects Satellite (CRRES) mission.[5] These satellite-based experiments were documented with optical data, which showed that the photoionized component of the barium cloud polarized and executed an $\boldsymbol{E} \times \boldsymbol{B}$ drift across the geomagnetic field. This drift was

Received 19 October 2001; revision received 27 June 2002; accepted for publication 30 August 2003.

*Research Associate, Laboratory for Atmospheric and Space Physics, CB 392 Duane Physics D135.
†Professor, Physics Department, Geophysical Institute, 903 Koyukuk Drive, P.O. Box 757320.
‡Research Scientist, Laboratory for Atmospheric and Space Physics, Mail Code 696.
§Assistant Group Supervisor, Space Department, 11100 Johns Hopkins Road. Member AIAA.
¶Branch Supervisor, Space Department, 11100 Johns Hopkins Road. Member AIAA.
**Deputy Director, 38 Leninsky Prospect, Building 1.
††Senior Scientist, Laboratory of the Magnetosphere-Earth Coupling, 38 Leninsky Prospect.
‡‡Head, Laboratory of the Magnetosphere-Earth Coupling, 38 Leninsky Prospect.

termed "skidding" by Huba et al.[6] Modeling efforts showed that the CRRES barium clouds skidded significantly farther than expected, suggesting a decoupling of the cloud from the momentum transferring Alfvénic disturbance. A likely consequence of this decoupling is a field-aligned electric field as suggested in Ref. 1.

More recently, the FLUXUS 1 and 2 aluminum injection experiments were conducted from rockets launched from Kapustin Yar, Russia, on 31 January 1997 (Ref. 7). In situ measurements recorded a diamagnetic cavity associated with the plasma jet,[8] and auroral emissions were observed.[9] The latter observation implies that enhanced electron fluxes existed near the cloud and were presumably associated with field-aligned currents caused by an Alfvénic disturbance.

As a continuation of the FLUXUS experiment, two aluminum shaped-charge releases were conducted from Poker Flat, Alaska, on 22 January 1999 as a part of the APEX North Star mission. In situ instrumentation provided plasma data at multiple points along the path of the plasma injection. The purpose of this paper is to present a comparison of plasma density, electric and magnetic field data with the results from a three-dimensional hybrid code simulation with an emphasis on understanding signatures that relate to the long-term (collisionless) dynamics of the plasma jet. The simulation provides a three-dimensional description of the electric fields, magnetic fields, and associated current systems to assist with the interpretation of the in situ measurements.

Summary of Observations

For completeness we provide a summary of the following relevant observations. A detailed overview of the experiment is provided by Erlandson et al.[10]

The first plasma injection from explosive-type generator 1 (ETG1) provided the best data for this study. The detonation occurred at an altitude of 363 km and was preceded by an air cloud to provide additional collisional ionization of the aluminum vapor. The resulting plasma jet, moving roughly perpendicular to the geomagnetic field, was highly localized with a peak density of roughly 10^9 cm^{-3}. The dense plasma slug created a diamagnetic cavity with a diameter of about 300 m (1–2 Al^+ gyrodiameters). The mean injection velocity was ~25 km/s perpendicular to $\boldsymbol{B}$. Three diagnostic payloads provided measurements for the ETG1 detonation: magnetometers on ETG2, magnetometers, electric field probes, a Langmuir probe on a plasma diagnostics payload (PDP), and another magnetometer on the optical sensor payload (OSP). The separation distances of these diagnostic payloads from ETG1 were 170 ± 10, 470 ± 10, and 1020 ± 10 m, respectively. All subpayload magnetometers recorded the passage of a diamagnetic cavity. The average velocity of the diamagnetic cavity between ETG2 and PDP was roughly 21 km/s, and between PDP and OSP the velocity was roughly 17 km/s indicating a slowdown of the plasma cloud (Fig. 1).

Figure 2 shows the Langmuir-probe data, total magnetic field, and three components of the electric field (coordinates defined in Fig. 3) measured at PDP. The total magnetic field is largely determined by δB_z, and so we use total B in Fig. 2 as a proxy for B_z in our analysis. The plasma density is clearly localized, and the diamagnetic cavity is nearly complete. At the leading edge of the cloud, the peak electric field is consistent with an $\boldsymbol{E} \times \boldsymbol{B}$ drift velocity of roughly 28 km/s, and the trailing edge peak has an $\boldsymbol{E} \times \boldsymbol{B}$ drift velocity of 18 km/s. Inside of the cavity the electric field goes to zero. Considerable wave activity is present in the electric field data at the leading edge of the cloud. Also, the magnetic field increases by about 10% prior to the diamagnetic cavity.

Plasma-Jet Ionosphere Coupling

One of the basic goals of the APEX North Star experiment was to address the interaction between the plasma jet and the space environment. Fundamental to plasma-jet ionosphere interaction is the transfer of momentum from the plasma jet, hereafter referred to as the "cloud," to the ambient ionospheric plasma. An Alfvénic disturbance, which propagates field-aligned currents into the ambient plasma, is generated by the injected plasma cloud (illustrated in the simulation results later). This current system decelerates the injected plasma cloud and accelerates the ambient medium thereby transferring momentum. A preliminary estimate of the momentum transfer can be made by assuming that the "frozen-in" condition of magnetofluids is valid, whereby we assume that the magnetic field lines can be treated as equipotentials and that ion-neutral and ion-electron collision times are much greater than the timescales of interest.

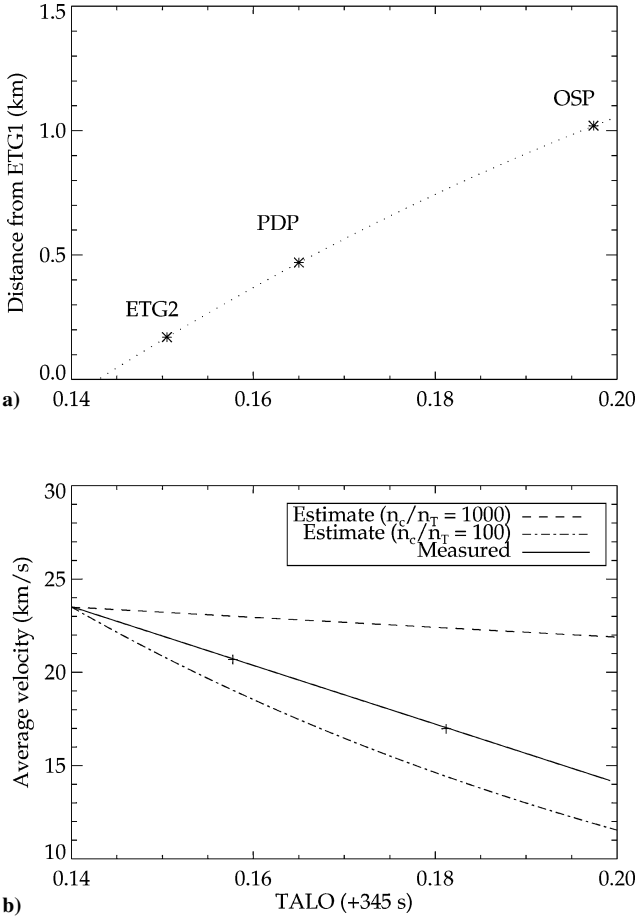

Fig. 1 Momentum transfer: a) location of the maximum δB_z associated with the diamagnetic cavity as a function of time (TALO = time after liftoff); b) average velocity of the diamagnetic cavity (——). Momentum transfer estimates for a cloud to ambient density ratio n_c/n_T of 1000 and 100 are also shown.

The change in the cloud's momentum is equal to the momentum transferred to the ambient plasma:

$$p_0 - p_c(t) = p_T(t) \tag{1}$$

where the subscript T refers to the transferred momentum and the subscript c refers to the aluminum cloud. The cloud's momentum as a function of time is

$$p_c(t) = n_c V_c m_c v_c(t) \sim n_c(AL) m_c v_c(t) \tag{2}$$

where n_c is the cloud density, m_c is the mass of the aluminum ions, V_c is the cloud volume with field-aligned extent L and cross-sectional area A, and $v_c(t)$ is the cloud velocity. If we assume that the local ambient plasma is accelerated up to v_c (plasma frozen to $\boldsymbol{B}$), then the total momentum in the volume of the magnetic flux tube bounded by the Alfvénic disturbance (i.e., Alfvén wing) is

$$p_T(t) = 2 n_T m_T \int v_c(t)(A v_A \, \mathrm{d}t) \tag{3}$$

where n_T and m_T are the ambient plasma (transfer medium) density and mass respectively, v_A is the Alfvén velocity, and A is the cross-sectional area of the magnetic flux tube subtended by the plasma

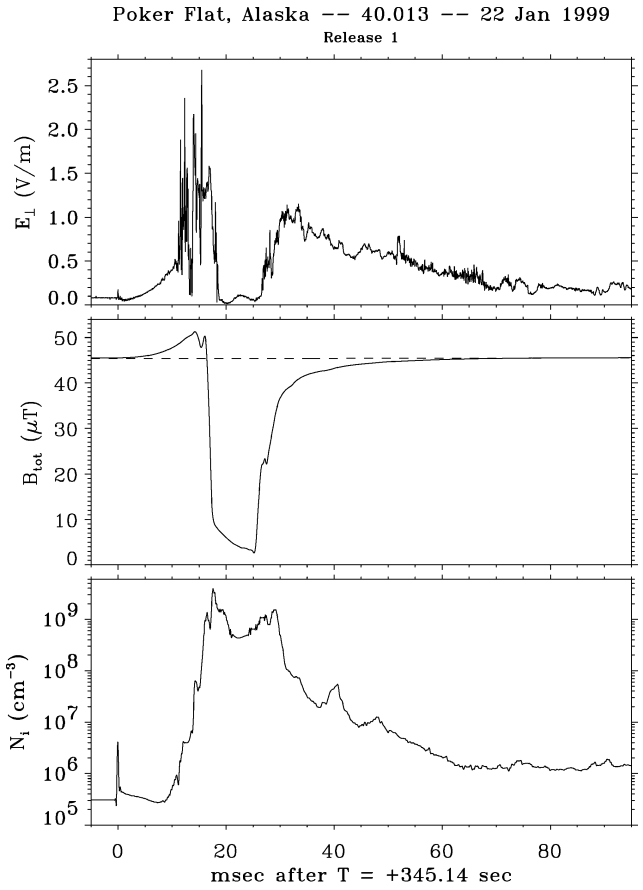

Fig. 2 In situ measurements from the plasma diagnostics payload of perpendicular electric field, total magnetic field, and plasma density.

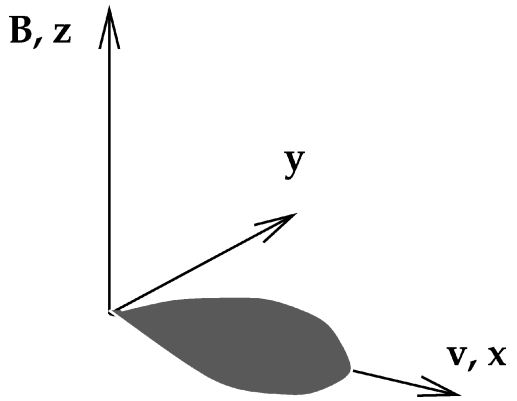

Fig. 3 Simulation coordinate system.

cloud. The factor of 2 accounts for upward and downward propagating disturbance. The rate of momentum transfer is

$$\frac{\mathrm{d}p_c(t)}{\mathrm{d}t} = -2n_T m_T A v_A v_c(t) \tag{4}$$

So the acceleration of the cloud is

$$\frac{\mathrm{d}v_c(t)}{\mathrm{d}t} = -\frac{2n_T m_T v_A}{n_c m_c L} v_c(t) \tag{5}$$

and the velocity of the cloud is

$$v_c(t) = v_0 e^{-t/\tau} \tag{6}$$

where $\tau = (n_c m_c L)/(2n_T m_T v_A)$ and v_0 is the initial velocity of the cloud.

A sample estimate is shown in Fig. 1 using the following parameters: $n_c/n_T = 100$ and 1000, $m_c/m_T = 27/16$, $v_A = 300$ km/s, $L = 300$ m, and $v_0 = 23.5$ km/s. The momentum transfer timescale τ is 0.084 s and 0.84 s for these parameters, respectively. The best fit to the measurements requires that $n_c/n_T = 150$. The peak density of the plasma cloud was 10^9 cm^{-3}. If we assume an average cloud density of 5×10^8 cm^{-3}, then the deceleration of the cloud is consistent with an ambient plasma density $\sim 3 \times 10^6$ cm^{-3}. The Langmuir-probe data showed that the ambient density was in fact one order of magnitude lower (2×10^5 cm^{-3}), and $n_c/n_T = 1000$ is consistent with the measurements. The magnetometer observations only cover the first 0.05 s of the cloud-ionosphere interaction, and the estimated momentum transfer timescale for $n_c/n_T = 1000$ is ~ 1 s; thus, it would be dangerous to draw conclusions regarding the long-term coupling. However, it appears initially that some anomalous braking occurred.

Hybrid Code

To further explore the cloud-ionosphere interaction, we have used a three-dimensional hybrid code to explore the quasi-steady-state configuration of the electric and magnetic fields of the APEX (i.e., $t < \tau$). Modeling the APEX plasma injection experiments requires the inclusion of both ion kinetic effects and the momentum coupling to the ambient plasma. This system involves size scales ranging from the ion gyroradius to Alfvén transit distances of several hundred kilometers. A hybrid code in which we treat the injected ions as fully kinetic particles, the ambient plasma as a fluid, and the electrons as a massless fluid, is a reasonable approach. This approach was first proposed by Harned,[11] and the particular algorithms for our code were developed by Swift[12,13] and Delamere et al.[1,14] The code assumes quasi-neutrality and is nonradiative. The equations of motion for the ion particles, the ambient ion fluid (O^+ is dominant ion species at an altitude of 363 km), the massless electron fluid, and the update of the electric and magnetic fields are described in this section.

The electric fields can be written explicitly from the electron momentum equation as

$$\boldsymbol{E} = -\boldsymbol{u}_e \times \boldsymbol{B} \tag{7}$$

where $\boldsymbol{E}$ is the electric field in units of ambient O^+ acceleration, $\boldsymbol{B}$ is the magnetic field in units of ambient O^+ ion gyro frequency, and $\boldsymbol{u}_e$ is the electron flow velocity. The total ion bulk flow velocity, $\boldsymbol{u}_i$ is given by

$$\boldsymbol{u}_i = (n_p/n)\boldsymbol{u}_p + (n_f/n)\boldsymbol{u}_f \tag{8}$$

where the subscripts p and f represent the particle and fluid constituents of the bulk flow.

The electron flow speed is evaluated from Ampere's law:

$$\boldsymbol{u}_e = \boldsymbol{u}_i - (\nabla \times \boldsymbol{B}_1)/\alpha n \tag{9}$$

where in mks units, $\alpha = \mu_0 e^2/m_{O^+}$ and where m_{O^+} is the fluid ion mass. The value of α is used to scale the simulation particle densities to their appropriate physical values. Note that $\boldsymbol{B} = \boldsymbol{B}_0 + \boldsymbol{B}_1$, where $\boldsymbol{B}_0$ is the ambient curl free geomagnetic field and $\boldsymbol{B}_1$ is the variable field.

Faraday's law is then used to update the first order magnetic fields:

$$\frac{\partial \boldsymbol{B}_1}{\partial t} = -\nabla \times \boldsymbol{E} \tag{10}$$

which upon using Eqs. (7) and (9) yields

$$\frac{\partial \boldsymbol{B}_1}{\partial t} = -\nabla \times \left[\left(\frac{\nabla \times \boldsymbol{B}_1}{\alpha n} - \boldsymbol{u}_i \right) \times \boldsymbol{B} \right] \tag{11}$$

With the equation for the magnetic fields written in this form, it can be shown that the first term on the right-hand side is responsible for the propagation of the whistler mode, and the second term, together with the particle/fluid equations, propagates the Alfvén modes.

Using Eqs. (7–9), the equation for ion particle motion is

$$\frac{d\boldsymbol{v}}{dt} = \boldsymbol{E}_p + \boldsymbol{v} \times \boldsymbol{B} \tag{12}$$

where $\boldsymbol{v}$ is the individual particle velocity and

$$\boldsymbol{E}_p = [(\nabla \times \boldsymbol{B}_1)/\alpha n - \boldsymbol{u}_i] \times \boldsymbol{B} \tag{13}$$

Similarly, the ion (O^+) fluid velocity is

$$\frac{\partial \boldsymbol{u}_f}{\partial t} = \boldsymbol{E}_f + \frac{n_p}{n}\boldsymbol{u}_f \times \boldsymbol{B} \tag{14}$$

where

$$\boldsymbol{E}_f = -(\boldsymbol{u}_f \cdot \nabla)\boldsymbol{u}_f + [(\nabla \times \boldsymbol{B})/\alpha n - (n_p/n)\boldsymbol{u}_p] \times \boldsymbol{B} \tag{15}$$

Note that the ordering of the terms in the expressions for $\boldsymbol{E}_p$ and $\boldsymbol{E}_f$ are different than in the expression for $\boldsymbol{E}$ given by Eqs. (7) and (9). This was done for the sake of computational convenience. Finally, the ambient fluid density was governed by

$$\frac{\partial n_f}{\partial t} + \nabla \cdot n_f \boldsymbol{u}_f = 0 \tag{16}$$

Simulation

The simulation was performed on a three-dimensional grid with $43 \times 33 \times 183$ grid cells. The APEX injections were made perpendicular to $\boldsymbol{B}$. The geomagnetic field, $\boldsymbol{B}_0 = 2 \times 10^{-5}\ T$, was taken in the z direction, the injection was in the x direction, and y completed the orthogonal coordinate system (Fig. 3). The observations of the plasma jet suggest an initial ion velocity distribution in spherical coordinates of the form

$$f(v_r, \theta, \phi) = N_0 e^{-(v_r - v_0)^2/v_{\text{th}}^2} e^{-\theta^2/\theta_0^2} \tag{17}$$

where θ is measured from the x direction, $N_0(10^{25})$ is the total number of released ions, v_0 (25 km/s) is the injection velocity, v_{th} ($\sqrt{}$20 km/s) is the thermal expansion velocity, and θ_0 (20 deg) is the characteristic cone angle of the beam. The ionization of the aluminum particles was considered complete at the beginning of the simulation run.

The grid cell dimensions in the release region were $0.5 \times 0.5 \times 0.5$ km, which was sufficient to resolve the ion gyromotion. The mass of a simulation ion was roughly four times the mass of an aluminum ion. The primary reason for using heavy ions was for computational feasibility. Aluminum ions would require grid cells of 0.1 km, and the Courant condition with respect to the propagation of the whistler mode required a time step that was a factor of 25 smaller. The qualitative results are sensitive only to the ratio of cloud size to ion gyroradius. For the parameters used in the simulation, the cloud dimension was roughly three simulation ion gyrodiameters, similar to the APEX aluminum cloud. Farther away from the release region, in the z direction, the grid spacing was increased to accommodate the large volume of ambient plasma that is coupled to the plasma cloud. The simulation was run until a quasi-steady-state configuration of the electric and perturbation magnetic fields was reached, which took less than the ion gyroperiod. Note that the PDP measurements were made at $t \sim 0.02$ s or $\sim\frac{1}{5}$ of the Al^+ ion gyroperiod, thus the comparison with the simulation results were made for $t < 1$ simulation ion gyroperiod. Energy and momentum were conserved to within 1%, and the simulation box was sufficiently large that the Alfvénic disturbance did not interact with the boundaries. Note that the E-region boundary will not affect the observations because the Alfvén propagation time (~1 s) is much larger than the time of the PDP measurements (~0.02 s).

Results and Discussion

The simulation results for steady state are shown in Fig. 4–8. Figures 4 and 5 show the electric fields and currents in the plane perpendicular to $\boldsymbol{B}$ along with the ion density. Figure 6 shows the total magnetic field in the yz plane, and Fig. 7 shows the currents in yz plane at the leading edge of the ion cloud. Figure 8 is intended for comparison with Fig. 2. The three panels in Fig. 8 show ion density, the y component of the electric field, and the z component of the magnetic field. Assuming a steady-state configuration of the electric and magnetic fields, profiles of these quantities were extracted from the simulation along the x direction. This approximates the measurements made at the PDP. The horizontal axis is 1) time for a point measurement made as the jet passes through and 2) distance for the jet moving from right to left at a given time.

The skidding distance of the ion cloud is caused by a combination of diamagnetism and polarization, which are both functions of density. For ion cloud densities greater than the ambient plasma density, the cloud polarizes, and $\boldsymbol{E} \times \boldsymbol{B}$ drifts (skids) in the injection direction. The polarization is caused by the difference between ion and electron gyromotion, and the associated electric field is in the y direction inside the cloud and dipolar outside the cloud. The quasi-neutrality approximation by definition precludes the formation of space charge layers, and the polarization is caused by an induction

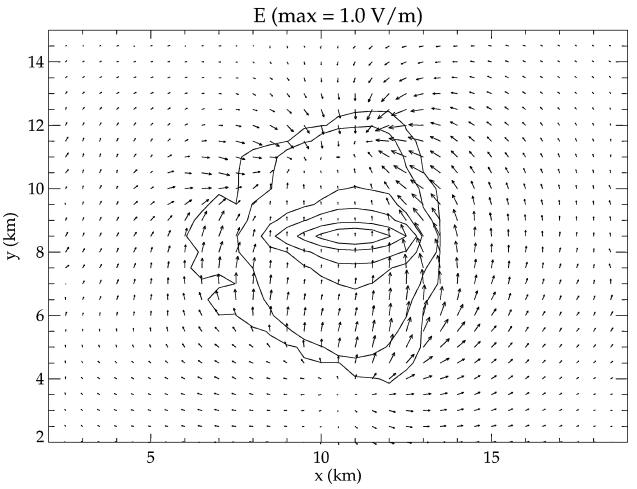

Fig. 4 Steady-state configuration of electric fields in a plane perpendicular to $\boldsymbol{B}$. The plasma cloud is indicated with density contours. The contour levels from outermost to innermost are 1×10^6, 1×10^7, 1×10^8, 2×10^8, 4×10^8, and 6×10^8 cm^{-3}. The outermost contour corresponds to the ambient plasma density.

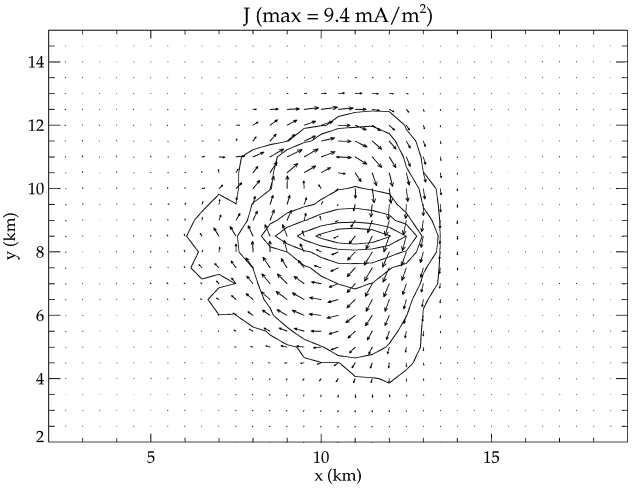

Fig. 5 Currents in a plane perpendicular to $\boldsymbol{B}$. This longitudinal current loop is responsible for the diamagnetic cavity. The ion cloud density contours are the same as noted in Fig. 4.

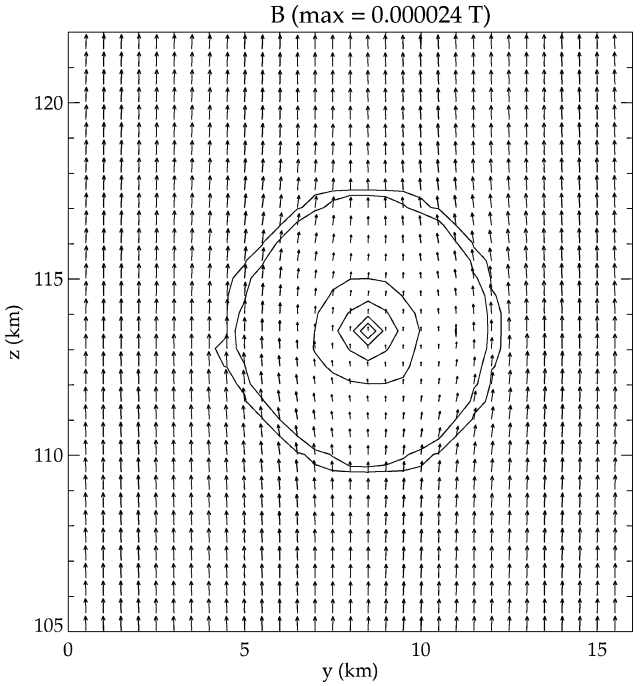

Fig. 6 Total magnetic field in the *yz* plane showing the diamagnetic cavity. The ion density contour levels are the same as in Fig. 4.

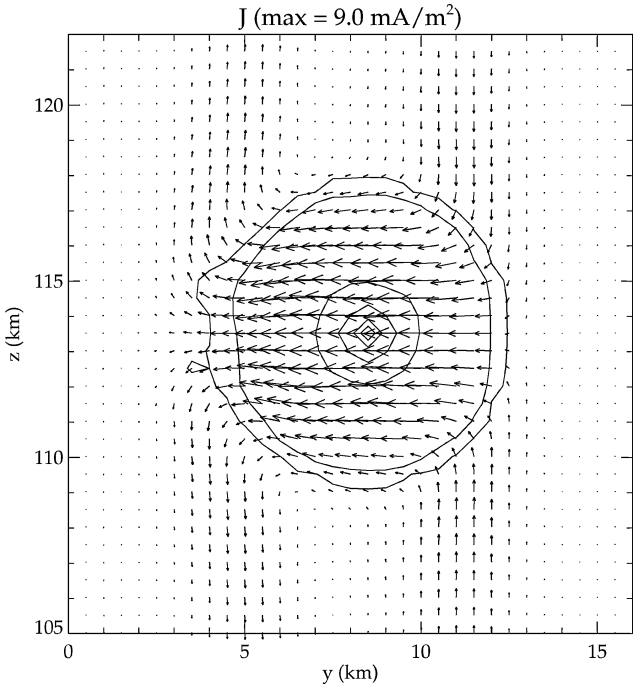

Fig. 7 Currents in the *yz* plane located toward the leading edge of the ion cloud. A portion of the cross-cloud current closes along the magnetic field as a part of the Alfvénic disturbance. The ion density contour levels are the same as in Fig. 4.

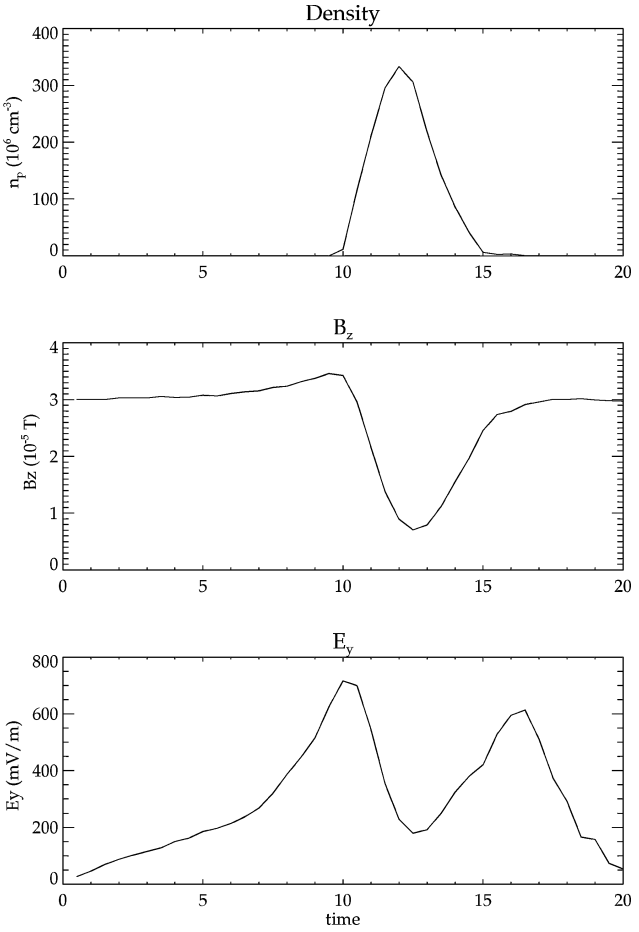

Fig. 8 Ion cloud profiles of density B_z and E_y. For the steady-state solution obtained in the simulation, the horizontal axis can be treated as time or distance. The horizontal axis is 1) time-for-point measurements made as the jet passes through and 2) distance for a jet moving from right to left at a given time.

electric field rather than an electrostatic electric field. The cloud can, nevertheless, be considered as a battery where the electrons form a negative terminal near $y = 11$ km in Fig. 4, and the ions form a positive terminal near $y = 4$ km. With respect to the electrons, the large ion gyroradius ($\sim$1400 m for $v = 25$ km/s) results in an asymmetry with respect to the center of the ion cloud. Notice that the positive terminal is displaced by an additional gyrodiameter away from the cloud center. The electric field within the cloud also decreases toward the negative terminal. This asymmetry is consistent with an asymmetry in the position of the diamagnetic cavity discussed next. A decrease in E_y is consistent with a decrease in B_z so that the ions maintain their injection velocity. As momentum is transfered to the ambient plasma, the cloud decelerates and momentum is conserved.

If the ion cloud density is sufficiently large, the particle pressure exceeds the geomagnetic field pressure and a diamagnetic cavity is formed. In the case of APEX, a nearly complete diamagnetic cavity was observed. The simulated cavity is not complete as the peak ion density is roughly a factor of 2 smaller than the observed peak density. (We elected not to generate a complete cavity for numerical reasons as a complete cavity generated considerable numerical noise.) The simulated cavity is not symmetric with respect to the cloud center. The center of the cavity is shifted toward the right (toward the negative charge layer). This asymmetry is again attributed to the large ion gyroradius.

The current systems consist of two components. The first component is a longitudinal (xy plane) current, which is responsible for the diamagnetic cavity. This diamagnetic current is generated by the density gradients at the boundary of the cloud. Figure 5 shows this longitudinal current loop along with its asymmetry with respect to the cloud center. The second current system is caused by the propagation of the Alfvénic disturbance. Figure 7 shows part of this current system flowing from right to left (negative to positive) in the leading edge of the cloud and closing along the magnetic field lines to the Alfvén wave fronts. The large currents seen in the leading edge of the cloud are essentially the superposition of the Alfvén current and the diamagnetic current. The currents shown in Figs. 5 and 7 are combined in Fig. 9 to illustrate the three-dimensional current system associated with the APEX experiments.

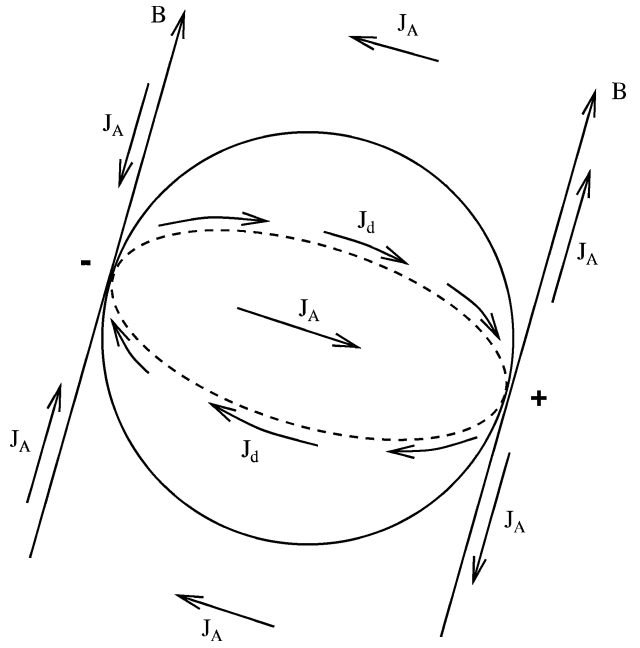

Fig. 9 Illustration of the APEX current system for motion into the page. The currents can be separated into contributions from the Alfvénic disturbance J_A and contributions from a longitudinal diamagnetic current J_d. The cloud is illustrated as a polarized sphere embedded within the geomagnetic field B.

The simulated cloud profiles shown in Fig. 8 are in good agreement with the in situ measurements. First, the diamagnetic cavity is offset to the right with respect to the peak ion density (i.e., trailing the peak ion density). The z component of the magnetic field increases by roughly 10% prior to the cavity, consistent with observation. Finally the electric field shows peaks at the leading and trailing edges of the ion cloud that are consistent with the observed E_y/B_z drift velocity of the ion cloud. The polarization electric field decreases in proportion to B_z as expected when quasi-neutrality is assumed. Note that the ratio of the peak electric fields, disregarding wave activity seen primarily at the leading edge of the cloud, is nearly the same as in the simulation. This suggests that a reasonable form of the initial ion velocity distribution was used.

The duration of the skidding ion cloud is unknown in the APEX experiment. However, the observed motion of the diamagnetic cavity during the early interaction ($t < 0.05$ s) shows that the cavity (dense plasma slug) slowed faster than our estimate for ideal magnetohydrodynamic coupling would predict. We attribute the deceleration of the dense plasma, slug to momentum transfer to the ambient plasma, which is exaggerated by rapid decay of the diamagnetic cavity as a result of the large ion gyroradius ("onion peeling"). The estimated momentum transfer timescale ($\sim$1 s), is much larger than the observation time (0.05 s), which precludes a definitive statement regarding the long-term plasma interaction of the aluminum ions with the ambient plasma. However, based on our comparison of observations with the hybrid code simulation it appears that the plasma cloud was fully coupled to the ambient plasma where we have associated the increase in B_z at the leading edge of the ion cloud with the Alfvénic coupling currents. One should not rule out the possibility that intense field-aligned currents could eventually lead to the formation of parallel electric fields causing momentum transfer limitations similar to CRRES. The observations of auroral emissions in the FLUXUS experiment suggest of the presence of parallel electric fields and electron acceleration.

Conclusions

A high-speed plasma jet was generated in the APEX North Star. The cloud was roughly 2–3 Al^+ gyrodiameters in size with a leading edge velocity of roughly 28 km/s and a trailing edge velocity of $\sim$18 km/s. This highly localized plasma slug was an excellent candidate for a hybrid code simulation because of scale lengths comparable with the ion gyroradius. Good agreement between in situ measurements of ion density, electric and magnetic fields, and the simulation results indicates that the cloud was fully coupled to the ambient plasma. However, the long-term interaction ($\sim$1 s) was not observed, and so a definitive statement regarding the momentum coupling cannot be made. Evidence of hot electron fluxes in the in situ spectral data and electron electrostatic analyzers suggests the presence of parallel electric fields that could be associated with the Alfvénic interaction.

References

[1]Delamere, P. A., Swift, D. W., Stenbaek-Nielsen, H. C., and Otto, A., "Momentum Transfer in the Combined Release and Radiation Effects Satellite (CRRES) Plasma Injection Experiments: the Role of Parallel Electric Fields," *Physics of Plasmas*, Vol. 7, No. 9, 2000, p. 3771.

[2]Connerney, J. E. P., Baron, R., Smith, T., and Owen, T., "Images of Excited H_3^+ at the Foot of the Io Flux Tube in Jupiter's Atmosphere," *Science*, Vol. 262, No. 5136, 1993, pp. 1035–1038.

[3]Clarke, J. T., Ballester, G. E., Trauger, J., Evans, R., Connerney, J. E. P., Stapelfeldt, K., Crisp, D., Feldman, P. D., Burrows, C. J., Casertano, S., Gallagher, J. S., III, Griffiths, R. E., Hester, J. J., Hoessel, J. G., Holtzman, J. A., Krist, J. E., Meadows, V., Mould, J. R., Scowen, P. A., Watson, A. M., and Westphal, J. A., "Far-UV Imaging of Jupiter's Aurora and the Io Footprint with the HST WFPC 2," *Science*, Vol. 274, No. 5286, 1996, pp. 404–409.

[4]Crary, F. J., "On the Generation of an Electron Beam by Io," *Journal of Geophysical Research*, Vol. 102, No. A1, 1997, pp. 37–50.

[5]Bernhardt, P. A., "Probing the Magnetosphere Using Chemical Releases from the CRRES Satellite," *Physics of Fluids B*, Vol. 4, No. 7, 1992, pp. 2249–2256.

[6]Huba, J. D., Mitchell, H. G., Fedder, J. A., and Bernhardt, P. A., "'Skidding' of the CRRES G-9 Barium Release," *Geophysical Research Letters*, Vol. 19, No. 11, 1992, pp. 1085–1088.

[7]Zetzer, J. I., Gavrilov, B. G., Kiselev, Yu. N., Rybakov, V. A., Gritshiv, V., Romanovsky, Y. A., Erlandson, R. E., Meng, C. I., and Stoyanov, B. J., "The Fluxus-1 and -2 Active Experiments: Investigation of Plasma Jet Dynamics and Interactions with the Ionosphere," *Spacecraft Charging and Technology Conference Proceedings*, 1999.

[8]Gavrilov, B. G., Podgorny, A. I., Podgorny, I. M., Sobyanin, D. B., Zetzer, J. I., Erlandson, R. E., Meng, C.-I., and Stoyanov, B. J., "Diamagnetic Effect Produced by the Fluxus-1 and -2 Artificial Plasma Jet," *Geophysical Research Letters*, Vol. 26, No. 11, 1999, pp. 1549–1552.

[9]Erlandson, R. E., Swaminathan, P. K., Meng, C.-I., Stoyanov, B. J., Zetzer, J. I., Gavrilov, B. G., Kiselev, Yu. N., and Romanovsky, Yu. A., "Observation of Auroral Emissions Induced by Artificial Plasma Jets," *Geophysical Research Letters*, Vol. 26, No. 11, 1999, pp. 1553–1556.

[10]Erlandson, R. E., Meng, C. I., Swaminathan, P. K., Kumar, C. K., Dogra, V. K., Stoyanov, B. J., Gavrilov, B. G., Kiselev, Y., Zetzer, J. I., Stenbaek-Nielsen, H. C., Lynch, K. A., Pfaff, R. F., Delamere, P. A., Bounds, S., and Gatsonis, N. A., "North Star Plasma-Jet Space Experiment," *Journal of Spacecraft and Rockets*, Vol. 41, No. 4, 2004, pp. 483–489.

[11]Harned, D. S., "Quasineutral Hybrid Simulation of Macroscopic Plasma Phenomena," *Journal of Computational Physics*, Vol. 47, 1982, pp. 452–462.

[12]Swift, D. W., "Use of a Hybrid Code to Model the Earth's Magnetosphere," *Geophysical Research Letters*, Vol. 22, No. 3, 1995, pp. 311–314.

[13]Swift, D. W., "Use of a Hybrid Code for Global-Scale Plasma Simulation," *Journal of Computational Physics*, Vol. 126, No. 0124, 1996, pp. 109–121.

[14]Delamere, P. A., Swift, D. W., and Stenbaek-Nielsen, H. C., "A Three-Dimensional Hybrid Code Simulation of the December 1984 Solar Wind AMPTE Release," *Geophysical Research Letters*, Vol. 26, No. 18, 1999, pp. 2837–2840.

D. L. Cooke
Guest Editor